

Remote sensing scoping study

Mapping burn severity of the Mt Midgeley Wildfire; Darkwoods Conservation Area

Seamus Murphy

May 2020

Introduction	2
Methods	3
Data sources	3
Results	4
Satellite imagery (2014, 2016, 2019)	5

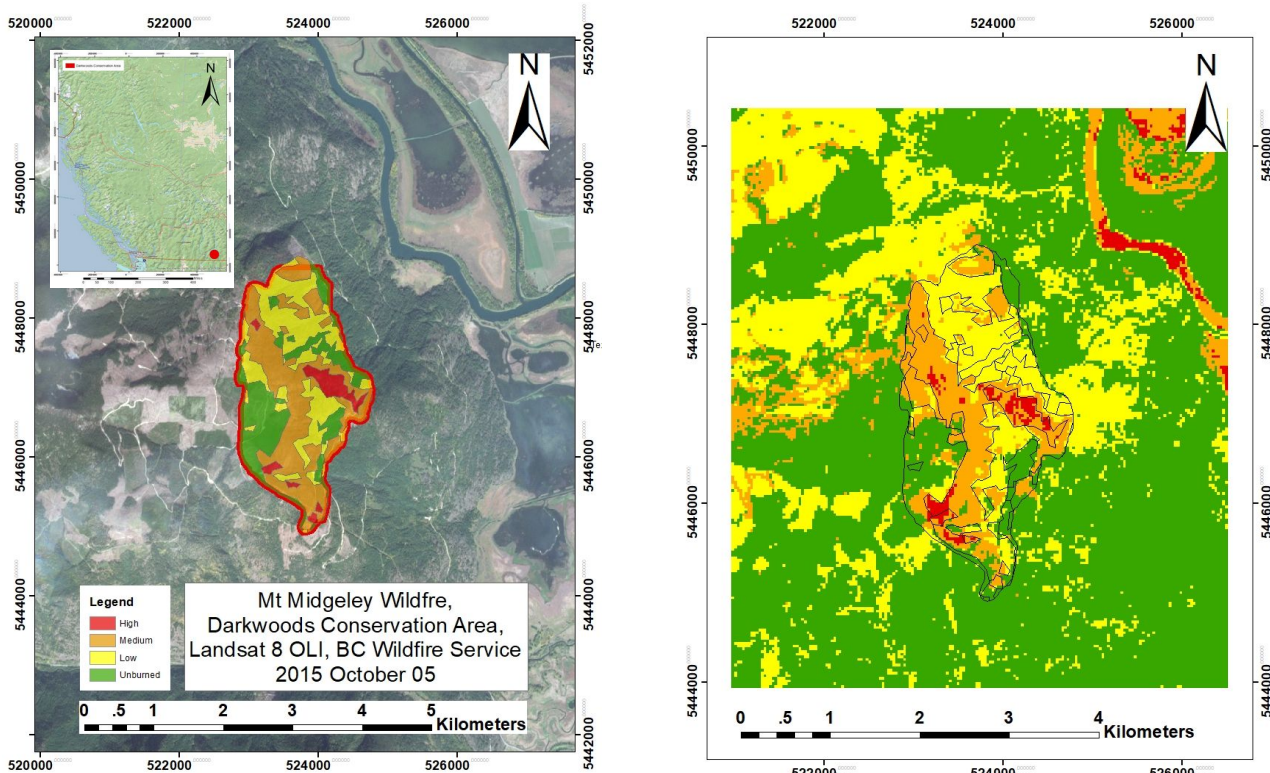
Remote sensing scoping study

Mapping burn severity of the Mt Midgeley Wildfire; Darkwoods Conservation Area

Introduction

The following report provides results from a remote sensing scoping study of the 2015 Mount Midgley Wildfire. The main aim of the study was to extract scoping information regarding the spatial distribution and severity of the fire remote sensing data generated from Landsat 8 satellite surveys (Table 1). The study also sought to test the accuracy of image classification algorithms and spectral indices for classifying wildfire burn across the site. A total of 13 spectral indices were tested (Table 2). These spectral equations were selected based on their sensitivities to wildfires in forest ecosystems, as demonstrated by previous studies of burn mapping and post-fire vegetation response (1–14).¹ Indexed images were stacked with simple vegetation band combinations (15) then classified separately using the Maximum Likelihood Classifier (MLC), the Support Vector Machine Learning (SVM), and the Random Tree Classifier (RTC) (16).² Finally, results were compared using accuracy tests based on kappa agreement. Results ranged between 0.0062 and 0.6035.

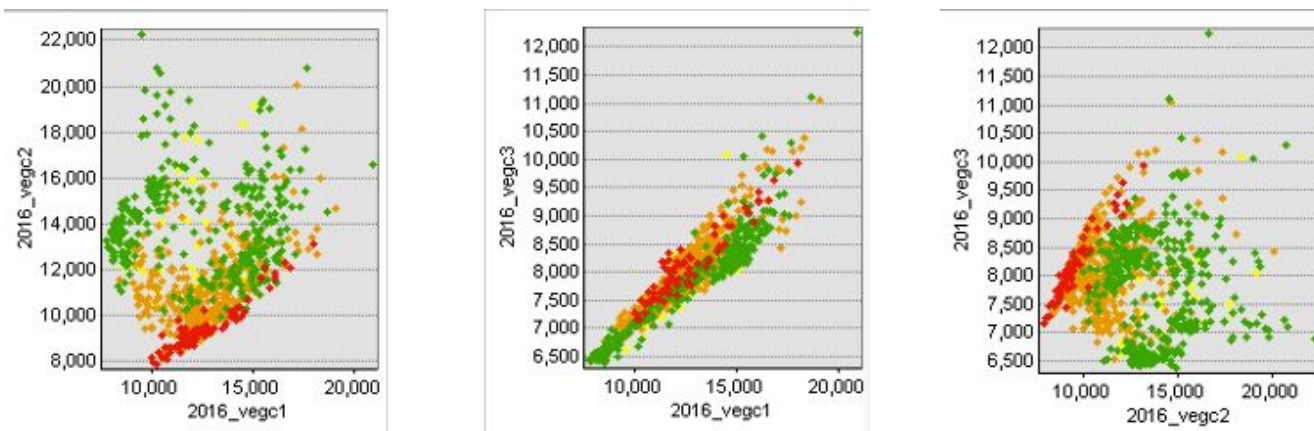
Burn severity classifications were provided by the BC Wildfire Service fire mapping documents (17) (Figures 1-2). According to the Kootenay Lake Fire Department, the wildfire event involved a mixed severity, stand-replacing fire. However, the BC Wildfire Service generated these wildfire maps remotely. Therefore, results should be considered incomplete. The site area was subsequently classified by the BC Wildfire Service according to four burn categories ("High", "Medium", "Low", "Unburned") (18). Using these geo-processed land designations, a supervised classification model was trained. With the supervised model as ground truth data, all 8 candidate spectral index models were compared for levels of accuracy.



Figures 1-2. Left: BC Wildfire Service Burn Severity Map. Right: Supervised classification of post-fire imagery based on training samples defined by BC WildFire Service

¹ The 13 spectral indices were chosen based on their documented application in studies of wildfire burns in forested landscapes. However, few of these studies included studies of wildfires at such smaller as the Mt Midgley wildfire site (439ha) (25). Even fewer studies involved examination of longer-term post-fire forest responses, documenting regrowth more than five years after wildfire occurrence (26).

² Processed images were stacked with multiband images comprised of vegetation analysis combinations (27)



Figures 3-5 VEG_2016 spectral signatures of burn severity based on land classifications trained by BC Wildfire Service Burn Mapping

Methods

The study site incorporates an area of 439ha that is located on the east side of Mt Midgley and 14km northwest of Creston, BC. Facing Kootenay Lake and Creston Valley, the site spans across elevations between 1,575m and 600m above seal level (a.s.l.).

Data from Landsat 8 were chosen due to its available longitudinal timescale. Landsat 8 dataset provided pre- and post-fire imagery of the site that matched source and acquisition data of the remote wildfire assessments conducted by the BC Wildfire Service³. Data from Sentinel 2A was selected for its high spatial resolution imagery (10m) that is recommended for post-fire assessments of small-scale sites (<1,000 ha; 1).

Data was analysed using ArcGis Map Software Version 10.7.1. Models were screened over two stages. Descriptive statistics and histograms were used to conduct first stage of model screening. This produced 8 ‘suitable models’ (Table 2) and 5 ‘failed models’ (Table 4). Second stage screening was based on accuracy assessment.

Due to constraints, the following report discussed results of image classification in relation to the remote wildfire severity sensing performance index (19). This index reported kappa values for best-performing indices as those ranging between 0.33 to 0.77 and elite indices ranging from 0.77 above.

Data sources

Table 1. Sources for the remote sensing data employed in the present study

Satellite data	Acquisition date	Spectral band	Spectral resolution (μm)	Spatial resolution (m)
Landsat 8	2014 July 01	B3. Green	(0.53-0.59)	30
	2016 June 27	B4. Red	(0.64-0.67)	30
	2019 Sept 01	B5. Near-Infrared	(0.85-0.88)	30
		B6. SW-Infrared1	(1.57-1.65)	30
		B7. SW-Infrared2	(2.11-2.29)	30
		B10. Thermal-IR1	(10.60-11.19)	100
		B11. Thermal-IR2	(11.50-12.51)	100

³ <https://catalogue.data.gov.bc.ca/dataset/fire-burn-severity-historical>

We estimated the effectiveness of 13 commonly used spectral indices to discriminate between burned and unburned areas. We expected that near-infrared based equations and the MSAV would provide positive results, though this was not the case. For vegetation analysis, the “Char Soil index” produced highest accuracy results. For burn analysis, the “Normalised Burn Ratio (B6)” produced highest accuracy results.

Table 2. Spectral indices employed in burn assessment of the 2015 Mt Midgeley Wildfire site

Label	Spectral index	Formula	Ref
1. CSI-Smith-B6	Char Soil Index (Band6)	= $\frac{NIR}{SWIR1}$	(2)
2. CSI-Smith-B7	Char Soil Index (Band7)	= $\frac{NIR}{SWIR2}$	(2)
3. BAI-Filipponi	Burn Area Index	= $\left(1 - \sqrt{\frac{NIR}{RED}}\right) * \left(\frac{SWIR2 - NIR}{\sqrt{SWIR2 + NIR}} + 1\right)$	(8)
4. MSAV-Qi	Modified Soil Adjusted Vegetation Index	= $\frac{2 * NIR + 1 - \sqrt{(2 * NIR + 1)^2 - 8 * (NIR - RED)}}{2}$	(9)
5. MIRBI-Trigg	Mid-InfraRed Burn index	= $10 * SWIR2 + 9.8 * SWIR1 + 2$	(10)
6. NBR-SWIR-Liu	Normalised Burn Ratio (Shortwave)	= $\frac{SWIR2 - SWIR1 - 0.02}{SWIR2 + SWIR1 + 0.1}$	(20)
7. NBR-Key-B6	Normalised Burn Ratio (Band6)	= $\frac{(NIR - SWIR1)}{(NIR + SWIR1)}$	(12)
8. NBR-Key-B7	Normalised Burn Ratio (Band7)	= $\frac{(NIR - SWIR2)}{(NIR + SWIR2)}$	(12)

Results

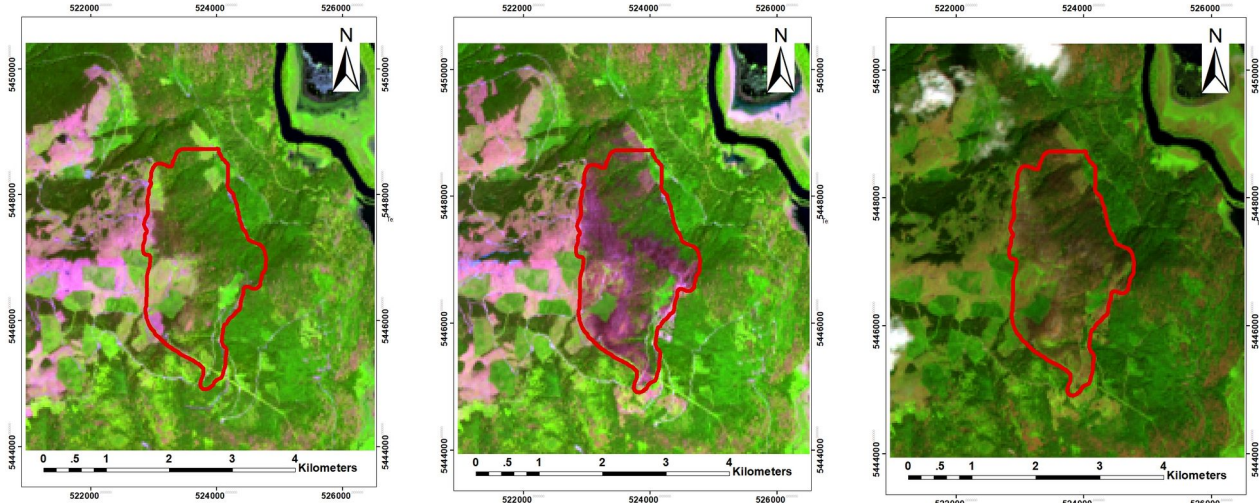
The study identified one high performing model for burn area identification ($K = 0.6035$) and one favourable for post-fire regrowth (0.2645). Table 3 shows results from surface level accuracy assessments of spectral indices. Results are ranked based on the K statistic of the confusion matrix generated between each spectral model and the ground truth image based on BC Wildfire Service classifications. From this, we find that NBR model was most effective. The NBR was originally developed to highlight reflectance of burned areas in large fire zones (21), however, here it was more effective than others in smaller scale fire sites. These present unusual findings, however, they will require field triangulation to discuss further.

Table 3. Accuracy assessments of spectral indices against BC Wildfire supervised image classifications

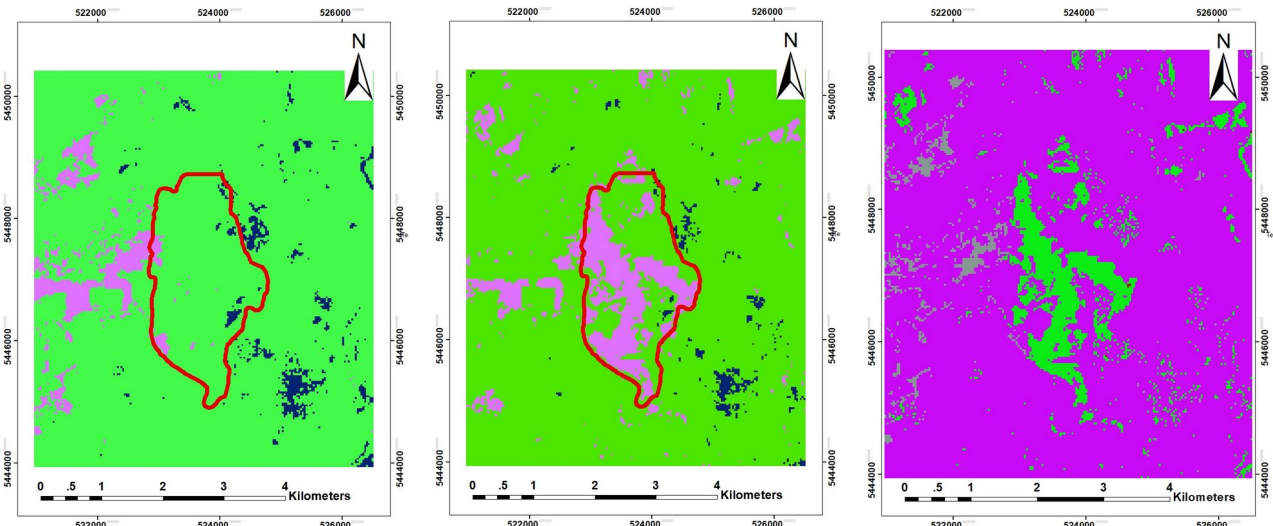
	Classes	Significant class	User accuracy	Kappa agreement	Accuracy Rank
1. CSI-Smith-B6	4	C1 (0.2202)	0.1924	0.0062	8
2. CSI-Smith-B7	4	C1 (0.3383)	0.1849	0.1050	6
3. BAI-Filipponi	4	C1 (0.9750)	0.7340	0.3271	3
4. MSAV-Qi	4	C2 (1.0000)	0.0120	0.0105	7
5. MIRBI-Trigg	4	C1 (0.9284)	0.7720	0.2645	4
6. NBR-SWIR-Liu	4	C1 (0.9146)	0.7280	0.1781	5
7. NBR-Key-B6	4	C1 (0.9439)	0.9180	0.6035	1
8. NBR-Key-B7	4	C1 (0.9044)	0.9040	0.3783	2

Spectral classifications of Mt Midgley Wildfire Site (2014, 2016, 2019)

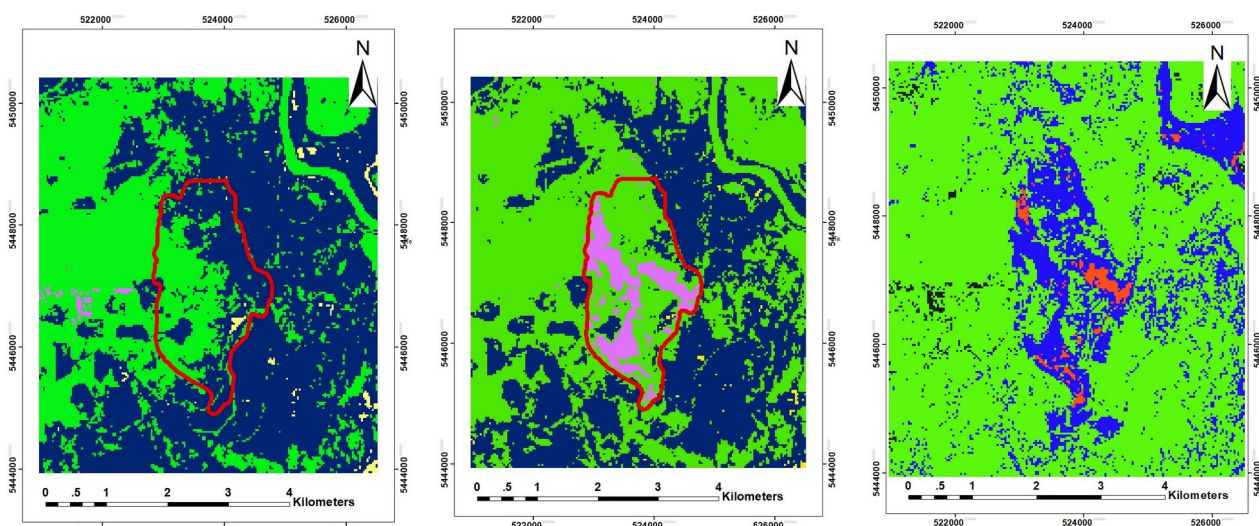
2014 (Pre-Fire) è è 2016 (Post-Fire) è è 2019 (Post-Fire)



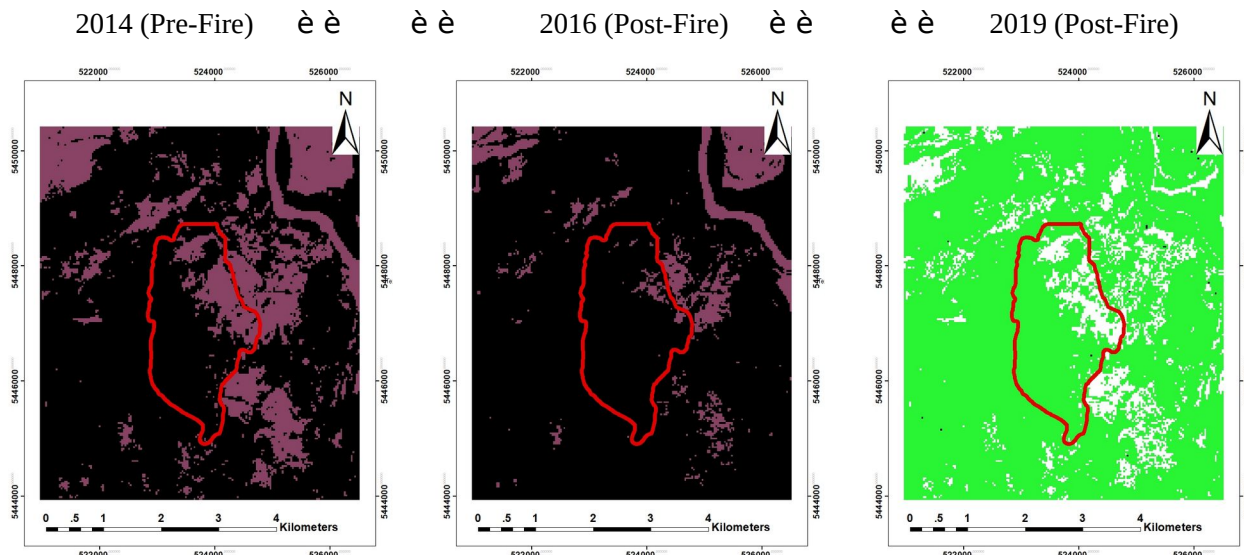
Figures 2-4 RGB imagery of vegetation change



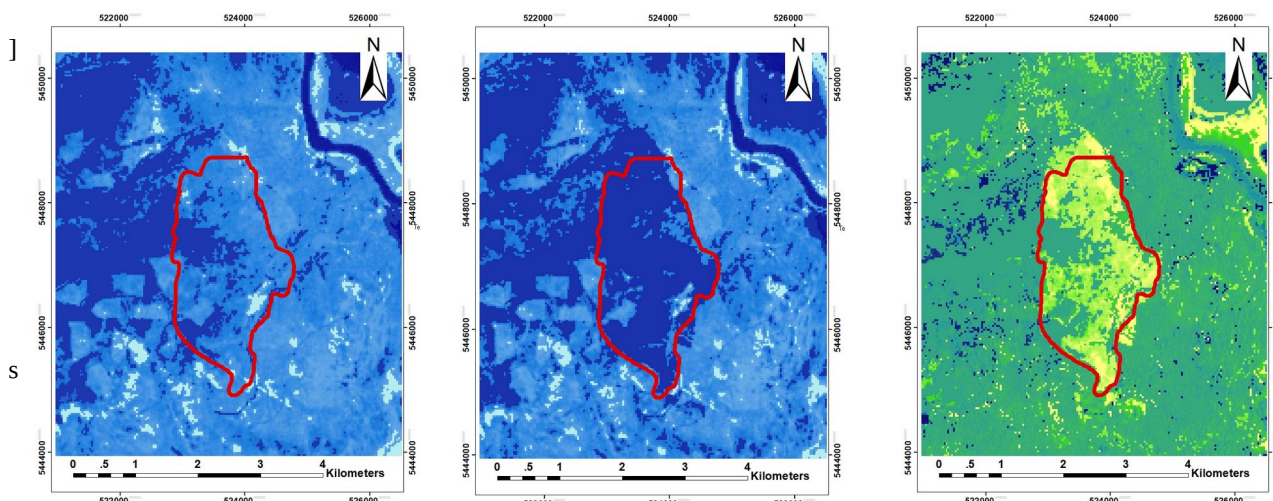
Figures 5-7 Char Soil Index B6 (Smith 1998)



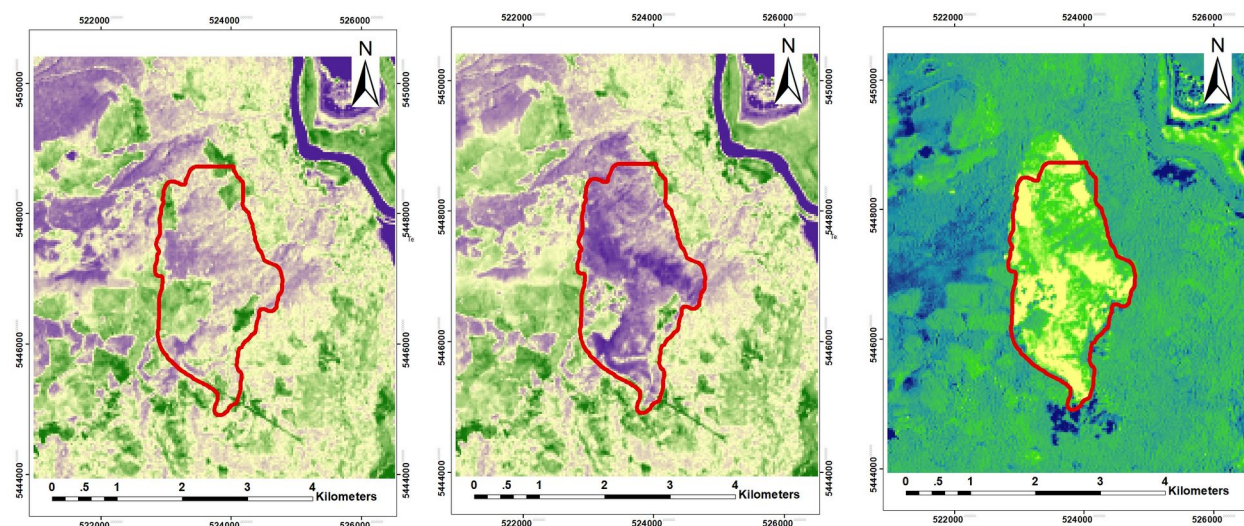
Figures 8-10 Char Soil Index B7 (Smith 1998)



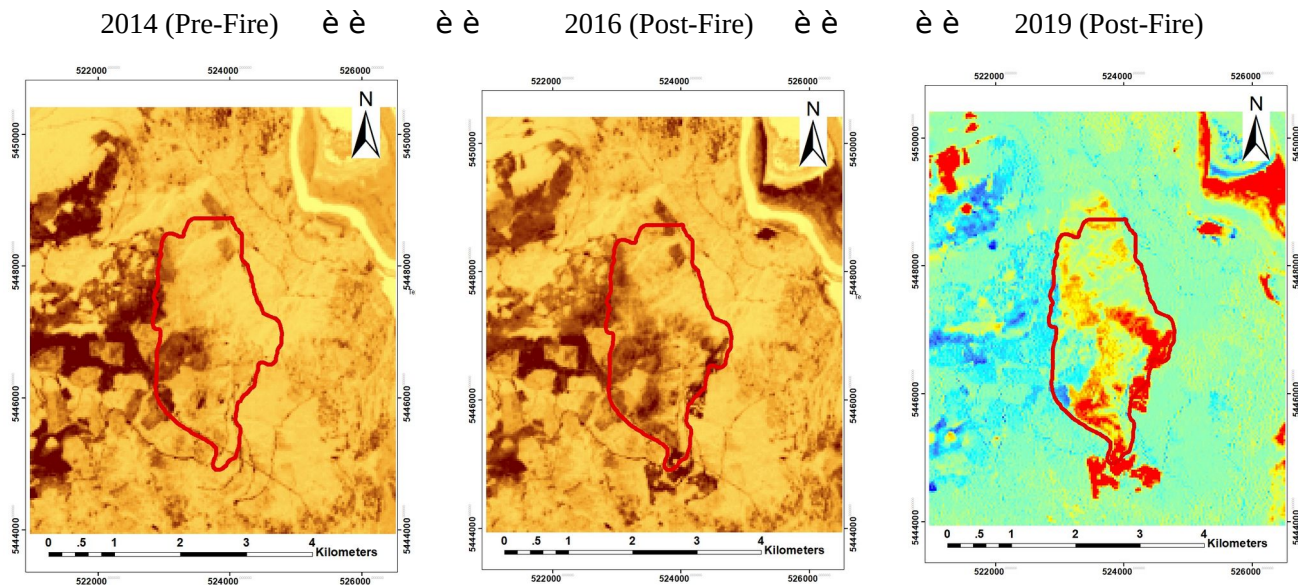
Figures 11-13 Burn Scar Index (Wang et al 2018)



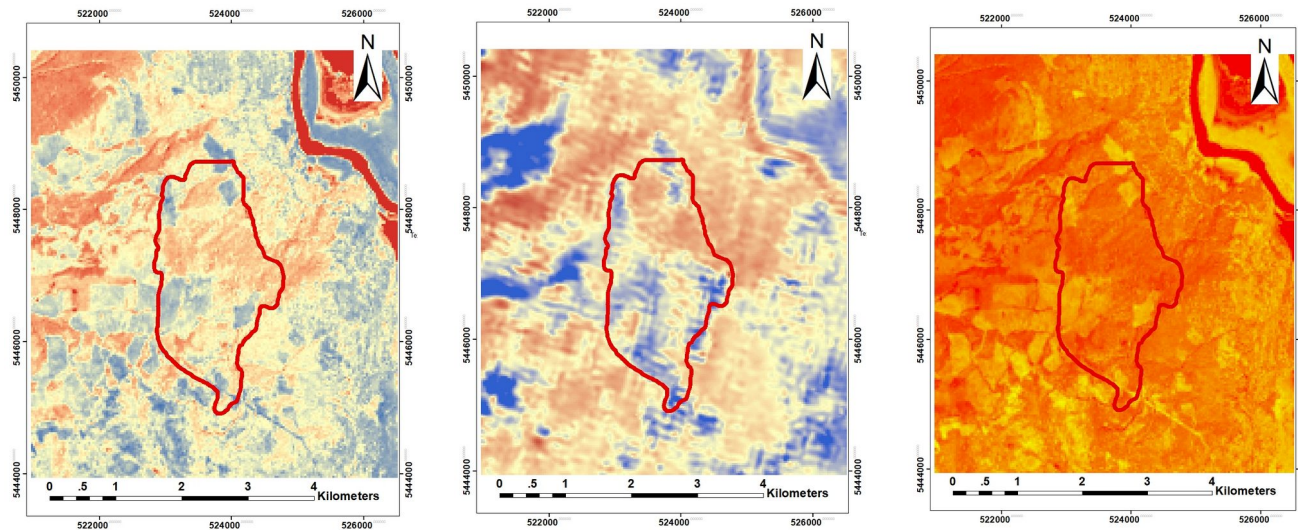
Figures 14-16 Burn Area Index (Filipponi et al 2018).



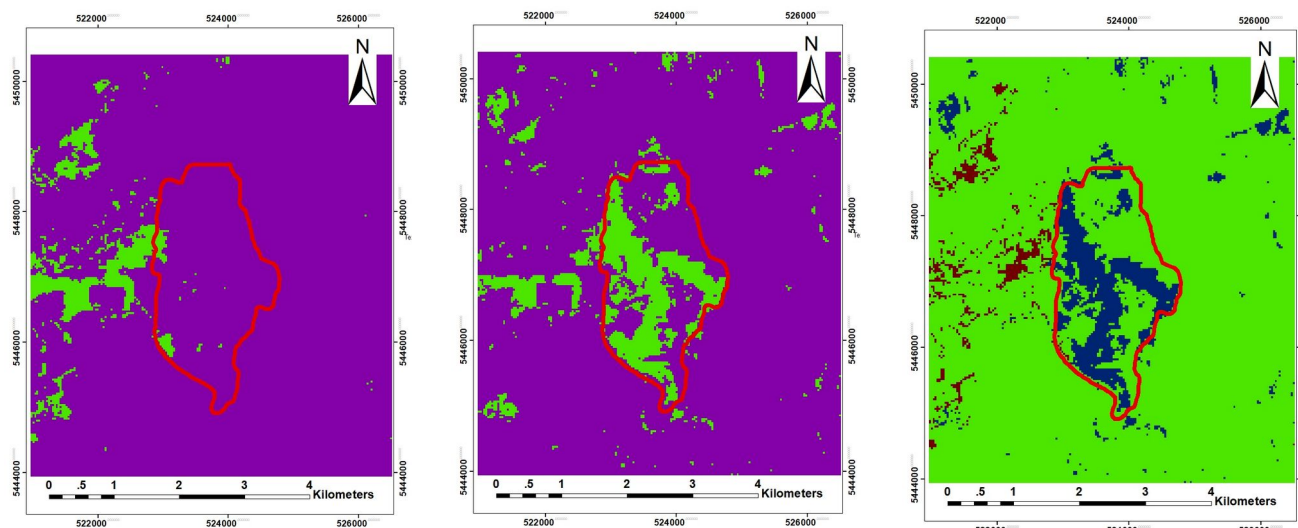
Figures 17-19 Modified Soil Adjusted Vegetation Index (Qi et al 1994)



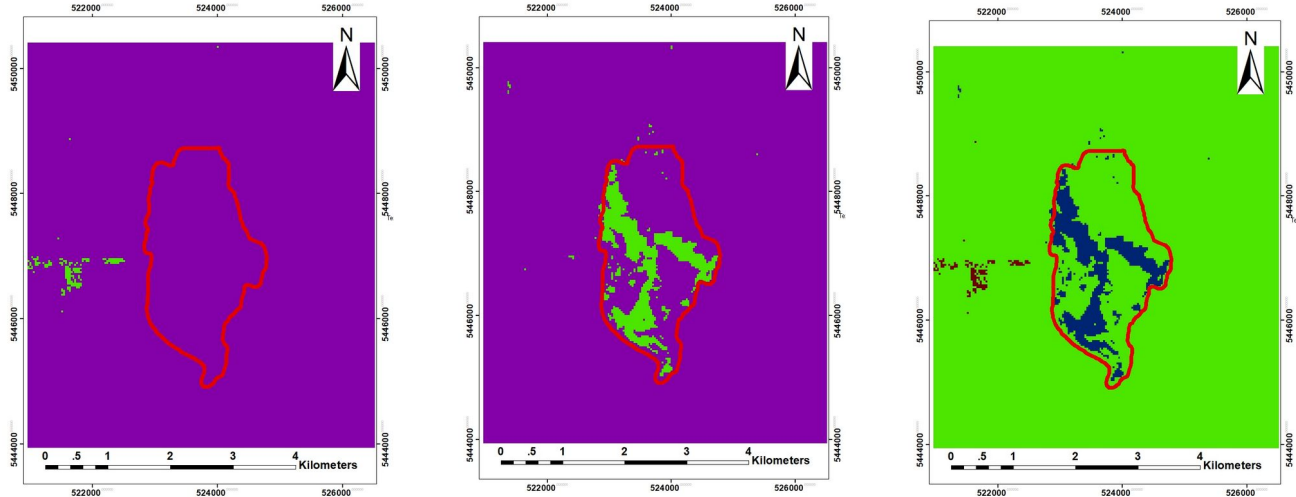
Figures 20-22 Mid-Infrared Burn Index (Trigg et al 2001)



Figures 23-25 Normalised Burn Ratio (Shortwavel Liu et al 2020)



Figures 26-28 Normalised Burn Ratio B6 (Key and Benson 2005)



Figures 29-31 Normalised Burn Ration B7 (Key and Benson 2005)

Table X. Failed models for burn assessment of 2015 Mt Midgeley Wildfire

Label	Spectral index	Formula	Ref
9. BSI-Wang	Burn Scar Index	$= \frac{(SWIR2 - RED)}{(SWIR2 + RED)(GREEN + RED + NIR)}$	(7)
10. BAI-Martin	Burn Area Index (1998)	$= \frac{1}{(0.1 - RED)^! + (0.06 - NIR)^!}$	(22-24)
11. NDVI-Rouse	Normalized Difference Vegetation	$= \frac{(NIR - RED)}{(NIR + RED)}$	(3,4)
12. NBRT-Holden	Normalised Burn Ratio - Thermal	$= \frac{(NIR - SWIR2) \left(\frac{TIR}{1000}\right)}{(NIR + SWIR2) \left(\frac{TIR}{1000}\right)}$	(5)
13. VIT6-Smith	Vegetation Index Thermal 6	$= \frac{(NIR - TIR)}{(NIR + TIR)}$	(1)

Bibliography

1. Smith A, Drake N, Wooster M, Hudak A, Holden Z, Gibbons C. Production of Landsat ETM+ reference imagery of burned areas within Southern African savannahs: comparison of methods and application to MODIS. *Int J Remote Sens.* 2007;28(12):2753–75.
2. Smith L. Use of Traditional Practices and Knowledge in Monitoring a Lake Malawi Artisanal Fishery. *North Am J Fish Manag.* 1998;18(4).
3. Rouse JW, Haas RH, Schell JA, Deering DW. Monitoring vegetation systems in the Great Plains with ERTS. *NASA Spec Publ.* 1974;351:309.
4. Tucker CJ. Red and photographic infrared linear combinations for monitoring vegetation. 1978;
5. Holden ZA, Smith AMS, Morgan P, Rollins MG, Gessler PE. Evaluation of novel thermally enhanced spectral indices for mapping fire perimeters and comparisons with fire atlas data. *Int J Remote Sens.* 2005;26(21):4801–8.
6. Burdon RD. Branching habit in radiata pine-breeding goals revisited. *New Zeal J For.* 2008;52(4):20.
7. Wang S, Baig MHA, Liu S, Wan H, Wu T, Yang Y. Estimating the area burned by agricultural fires from Landsat 8 Data using the Vegetation Difference Index and Burn Scar Index. *Int J Wildl Fire.* 2018;27(4):217–27.
8. Filippioni F. BAIS2: Burned Area Index for Sentinel-2. In: Multidisciplinary Digital Publishing Institute Proceedings. 2018. p. 364.
9. Qi J, Chehbouni A, Huete AR, Kerr YH, Sorooshian S. A modified soil adjusted vegetation index. 1994;
10. Trigg S, Flasse S. An evaluation of different bi-spectral spaces for discriminating burned shrub-savannah. *Int J Remote Sens.* 2001;22(13):2641–7.
11. Lu R, Zhao X, Li J, Niu P, Yang B, Wu H, et al. Genomic characterisation and epidemiology of 2019 novel coronavirus: implications for virus origins and receptor binding. *Lancet [Internet].* 2020;395(10224):565–74. Available from: [http://dx.doi.org/10.1016/S0140-6736\(20\)30251-8](http://dx.doi.org/10.1016/S0140-6736(20)30251-8)
12. Key CH, Benson NC. Landscape assessment: remote sensing of severity, the normalized burn ratio and ground measure of severity, the composite burn index. FIREMON Fire Eff Monit Invent Syst Ogden, Utah USDA For Serv Rocky Mt Res Stn. 2005;
13. Kohler A, Rinaldi C, Duplessis S, Baucher M, Geelen D, Duchaussoy F, et al. Genome-wide identification of NBS resistance genes in *Populus trichocarpa*. *Plant Mol Biol.* 2008;66(6):619–36.
14. Lukacs PM, Burnham KP, Anderson DR. Model selection bias and Freedman's paradox. *Ann Inst Stat Math.* 2010;62(1):117.

15. Yan H, Bi H, Li R, Eldridge R, Wu Z, Li Y, et al. Assessing climatic suitability of *Pinus radiata* (D. Don) for summer rainfall environment of southwest China. *For Ecol Manage.* 2006;234(1–3):199–208.
 16. Richards JA, Richards JA. *Remote sensing digital image analysis*. Vol. 3. Springer; 1999.
 17. Service M of FL and NROBW. 15 N 70624 Fire Perimeter. 2015.
 18. Park J, Ko B, Nam J-Y, Kwak S. Wildfire smoke detection using spatiotemporal bag-of-features of smoke. In: 2013 IEEE Workshop on Applications of Computer Vision (WACV). 2013. p. 200–5.
 19. Tran BN, Tanase MA, Bennett LT, Aponte C. Evaluation of spectral indices for assessing fire severity in Australian temperate forests. *Remote Sens.* 2018;10(11):1680.
 20. Liu S, Zheng Y, Dalponte M, Tong X. A novel fire index-based burned area change detection approach using Landsat-8 OLI data. *Eur J Remote Sens.* 2020;53(1):104–12.
 21. Garcia MJL, Caselles V. Mapping burns and natural reforestation using Thematic Mapper data. *Geocarto Int.* 1991;6(1):31–7.
 22. Chuvieco E, Martin MP, Palacios A. Assessment of different spectral indices in the red-near-infrared spectral domain for burned land discrimination. *Int J Remote Sens.* 2002;23(23):5103–10.
 23. Martin M. *Cartografía e inventario de incendios forestales en la Península Ibérica a partir de imágenes NOAA-AVHRR*. Universidad de Alcalá; 1998.
 24. Luca C, Sara P, Angelino CV, Nicomino F, Ullo S, Pia A. Post-fire assessment of burned areas with very high resolution Sentinel-2 and Landsat-8 images. In: GEOBIA 2018. 2018.
 25. Meng R, Wu J, Zhao F, Cook BD, Hanavan RP, Serbin SP. Measuring short-term post-fire forest recovery across a burn severity gradient in a mixed pine-oak forest using multi-sensor remote sensing techniques. *Remote Sens Environ.* 2018;210:282–96.
 26. Sparks AM, Kolden CA, Talhelm AF, Smith A, Apostol KG, Johnson DM, et al. Spectral indices accurately quantify changes in seedling physiology following fire: towards mechanistic assessments of post-fire carbon cycling. *Remote Sens.* 2016;8(7):572.
 27. Li P, Jiang L, Feng Z. Cross-comparison of vegetation indices derived from Landsat-7 enhanced thematic mapper plus (ETM+) and Landsat-8 operational land imager (OLI) sensors. *Remote Sens.* 2014;6(1):310–29.
- .

Data collection plan

Mapping post-fire conifer seedlings in the Darkwoods Conservation Area

June 10

Introduction:	2
Methods; Study design	4
Methods; Data collection	4
Methods; Variables	5
Appendix I: Data collection forms	8
Appendix II; Composite burn criteria	8
Bibliography	9

Expected outputs:

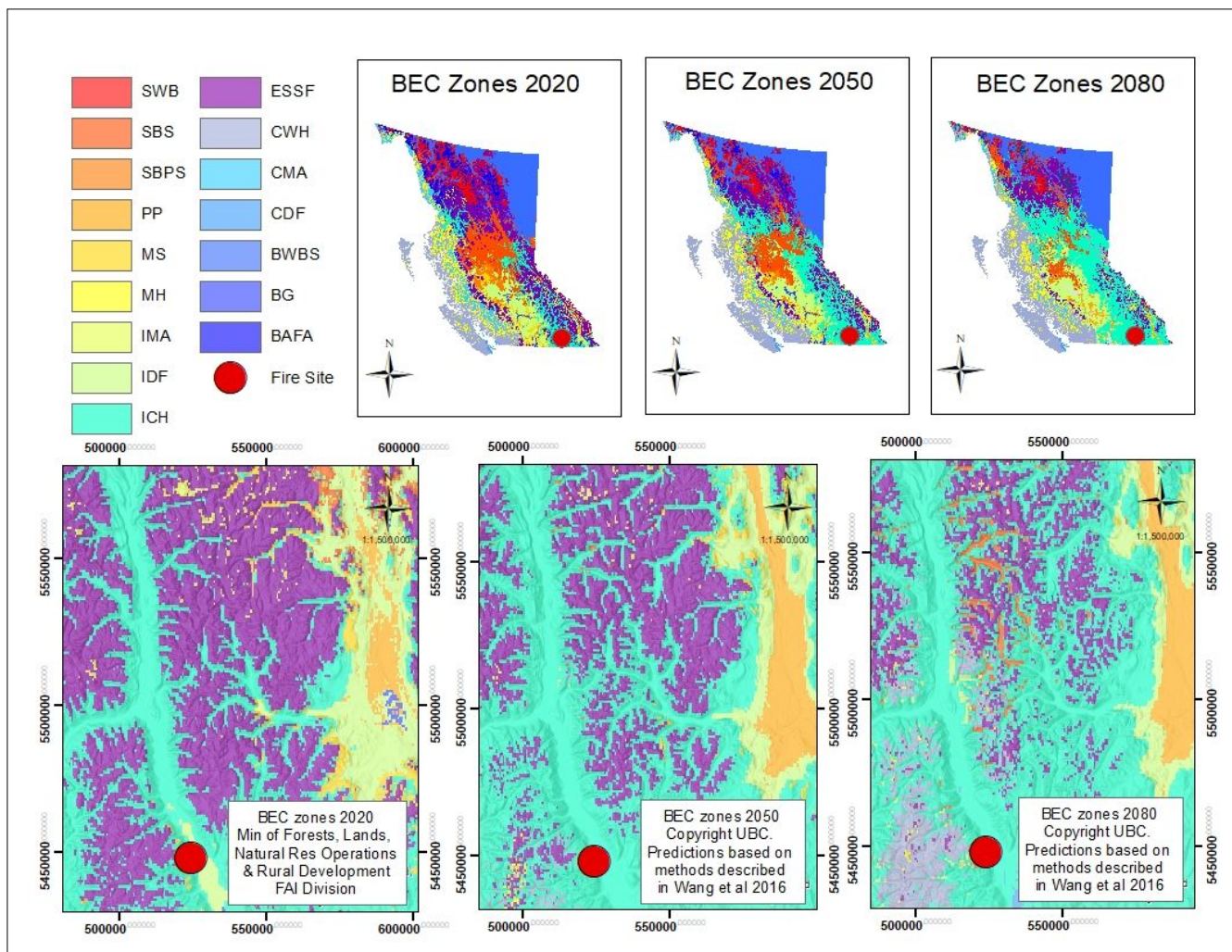
Spatial patterns of conifer regeneration following mixed-severity fire; Importance of seed source, topography and climate to species distribution and biogeoclimatic ecosystem shifts

Evaluation of machine learning classifiers and spectral indices in fire severity mapping of the Darkwoods Conservation Area

Introduction:

In southern and interior British Columbia, recent climatic variations have been linked to increasing forest disturbances caused by wildfire activity that have impacted negatively on reforestation (1–4) and natural tree regeneration (5–7). In the subalpine forests of the Selkirk Mountains, many tree species have evolved in concert with natural wildfire regimes through the development of fire-related regeneration strategies that depend on early and abundant post-fire seedling establishment (8). Therefore, the combined effects of altering wildfire activity and increasing drought pose a serious threat to these conifer trees (9–11). In response, a growing number of studies is examining the distribution and spatial arrangement of post-fire seedlings as a key indicator of climate-induced ecosystem shifts (12–18).

Within the Kootenay Lake region surrounding the Mt Midgley study site, research suggests biogeoclimatic shifts are likely to impact the forest ecosystems of AT, ESSF and ICH (Figures 1¹) As higher elevation envelopes (ESSF and AT) retreat further higher and northwards, Interior Cedar-Hemlock is expected to throughout the current study site, which will contribute to range expansions among Western larch, Douglas-fir, ponderosa pine, Western redcedar and Western hemlock, and range reductions among Engelmann spruce, lodgepole pine and higher elevation conifers (2,19,20).



Figures 1: Predictive ecosystem mapping of British Columbia's forests, 2020-2080 (Wang et al (2016, 21)

¹ For full review see (2). For BEC classifications see (15,76,77)

However, research also suggests these outcomes will differ for different conifer species due in part to their variable fire-related regenerative strategies (6,12,22). For instance, regeneration mechanisms differ widely between fire ‘avoiders’ (engelmann spruce), fire ‘invaders’ (douglas-fir, western larch, ponderosa pine), and fire ‘evaders’ (seritonous lodgepole pine) (8). On the one hand, regeneration of fire ‘invaders’ is dependent on nearby seed source and will therefore respond negatively to increasing burn area. On the other, since regeneration among fire ‘evaders’ is conducted through more distant dispersal mechanisms, the distance to patch edge is likely less significant.

Meanwhile, in these mountainous landscapes, topography provides another key driver of this change (23–28). Depending on slope, aspect and elevation, site micro-topography can impact on tree regeneration either positively through geomorphic sheltering or negatively by increasing climatic exposure. In post-fire settings, research notes the significance of aspect on seedling establishment of western redcedar and western hemlock (29), ponderosa pine and douglas-fir (30), and western larch (31).

and
the

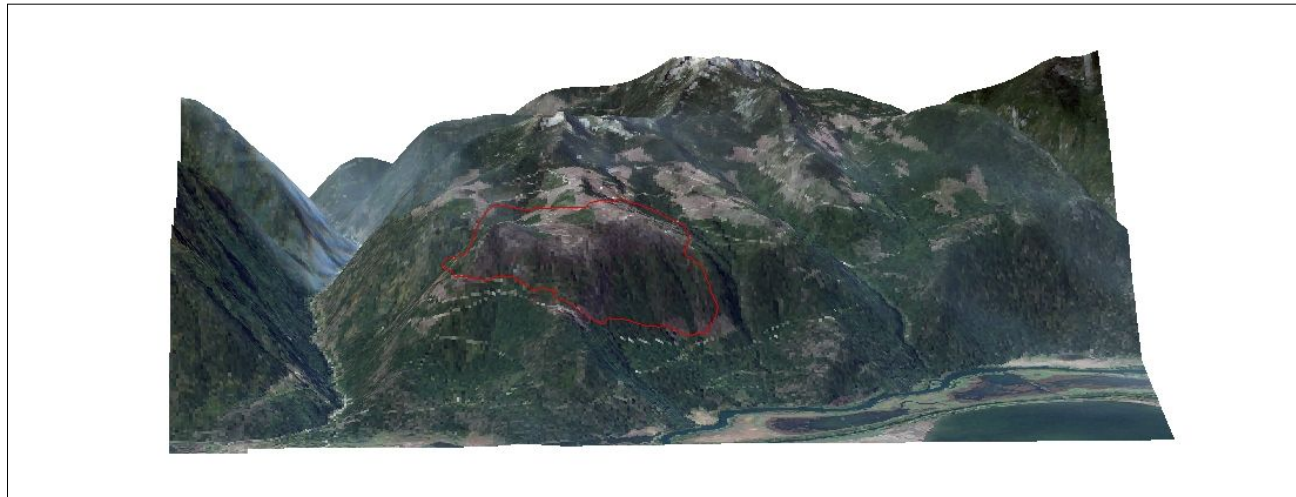


Figure 1
Study area

Despite this being a key area of research, there remains a scarcity of data on natural seedling establishment and an even greater deficit on post-fire tree regeneration across Canada (13,15,35–37). As a result, many climate change studies have failed to incorporate seedlings into species distribution models and have thus been limited in their predictions of species responses to climate variations. In response, this study will map the density and spatial arrangement of post-fire seedlings among seven conifer species in three biogeoclimatic ecosystem subzones. The main aims of the study are to identify patterns of tree regeneration, to examine how seedling patterns are responding to variable seed source, topography, climate, and burn severity, and to understand how these factors vary for different conifer species in different biogeoclimatic subzones. Specifically, the study will test the following three hypotheses:

- 1) Higher post-fire seedling densities, height and aggregated spatial patterns of each will be found closer to residual parent trees for fire avoiders and invaders, but not fire evaders.
- 2) Higher post-fire seedling densities, height and aggregated spatial patterns of each will be found in more mesic topographic gradients for western larch, engelmann spruce, western redcedar and western hemlock, but not for douglas-fir, ponderosa pine & lodgepole pine.
- 3) These factors impact variably on the post-fire regeneration of different conifer species in different BEC zones.

Methods; Study design

Spatial patterns of post-fire tree regeneration in the Pacific Northwest have long been the subject of forest research (38,39,48–50,40–47). This work involved important breakthroughs in quantitative methods that enabled the advancement of seed dispersal models and patch analysis, namely point-pattern analysis (17,18,51–54). In this study, we will employ both global and local point pattern analyses to assess the regeneration patterns of each species. Through stem-point mapping, we will examine if seedling densities deviate from complete spatial randomness assumptions according to location-dependent, distance-dependent and covariates of interest (51, Table 2).

Using a point-quadrat- and point-grid sampling design, four 2ha-plots (141x141m) will be established between fire severity patches and biogeoclimatic zones (Figure 3). Two plots will be located in the lower ICH subzone and two plots will be established in the upper ESSF subzone. Two of these plots will be located in moderate-to-high burn severity sites and two will be established in the low-burn severity sites. Delineation of biogeoclimatic ecosystem ranges was mapped using the 2017 BEC geo-dataset (56). According to these delineations (Figure 4), the study site was divided fairly evenly between three BEC zones: ESSFfwm4 (207.63ha, 43.28%), ICHdw1 (187.42ha, 39.07%), and ICHmw4 (84.72ha, 17.69%).

Methods; Data collection

Field measurements

At plot centres, x, y, z reference points will be established using GPS coordinates (UTM NAD83 Zone 11N) and compass azimuth. In each plot, the spatial location, elevation, species, and heights of all post-fire conifer seedlings (<32cm) will be measured from plot reference points using a range finder, tape and compass. A threshold height for post-fire (2015) seedling height will be set at 32cm following reports of maximum annual seedling growth ranging from 8cm to 45cm between Engelmann spruce and Douglas-fir (57–60). In dense clusters of similar species with similar height, the central location, mean height and number of stems will be measured. Distance to pre-fire seed source was be measured based on supervised classification of pre-fire forest inventory derived from 250m satellite imagery (Table 1, Figure 3, Ref: 60).Topographic variables will be generated for each cell (30m) using a 7.5s digital elevation model: slope, aspect, elevation and a terrain ruggedness index. This data was classified into eight classes (Table 1, Figure 4), indicating high levels of exposure and steep inclines throughout most of the site ($>16^\circ$, 530m - 1,800m a.s.l.). However, as the site slopes down to the valley floor, it provides a favourable east- and north-east facing aspect that has potential for geomorphic sheltering. Due to the particular significance of the site's orientation and slope, a Ruggedness Index (RIX) was added as an explanatory variable. Using a simple, geographically weighted regression, RIX values were estimated as the mean of the absolute differences in elevation between each point and its immediate neighbouring grid of cells. Based on the neighbourhood factor of 3 x 3, RIX values were assigned to each cell. Lower values indicated mesic, flat areas and higher values indicated highly exposed 'rugged' areas such as ridges (62,63, Figure 5).

Climate data

Climate data were acquired from three sources: the ClimateNA platform ², NASA's surface meteorology and solar energy database,³ and the Global Wind Atlas.⁴ This included monthly values of minimum, mean and maximum temperature, precipitation, and solar radiation obtained from ClimateNA, and daily wind values derived from NASA. To represent climatic variations across site elevations, climate data were fitted with the digital elevation file using the original Parameter elevation on Independent Slopes regression (PRISM) (64). Somewhat similar to calculations above, climatic values were geographically weighted using instead the neighbouring parameters of elevation above sea level, slope, aspect and latitude. This was done using a local kernel function based on a distance-dependent Gaussian weighting scheme with parameters set

² http://www.climatewna.com/help/ClimateNA/Help.htm#_Toc410137604

³ <https://power.larc.nasa.gov/docs/methodology/>

⁴ <https://globalwindatlas.info/about/method>

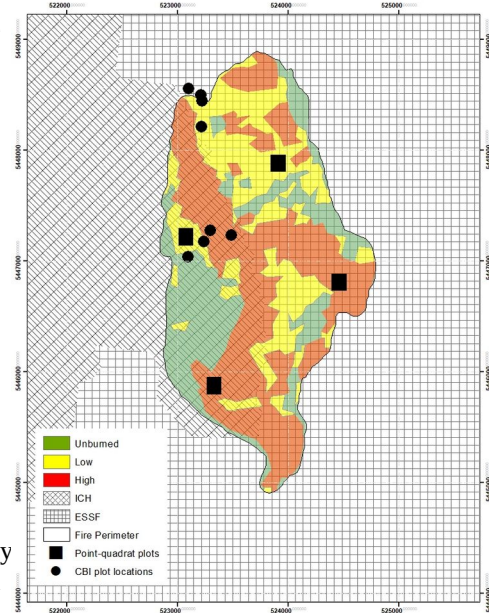


Figure 3, Point-sampling design

by global positioning coordinates (2,21,65). With the GTDEM 7.5s 250m digital elevation map, newly derived conditional estimates provided mean values for voxels 1x1km resolution (Table1, Figure 5). In order to assess the affect of climatic variations on seedling establishment, post-fire values of mean monthly temperature (2015-2019) were compared with baseline climatic ‘normals’. A baseline was derived from data recorded during the 30-year period of 1981 to 2011.

Differences in absolute monthly mean estimates were standardized using standard deviation of reference period and presented as Comparing against the baseline, post-fire temperature changes were calculated

Fire-severity data

Burn severity field plots were measured following the Composite Burn Index (CBI) and methodology outlined by the BC Ministry of Forests, Lands and Natural Resource Operations (66,67). The CBI tool assesses burn effects across five strata along the forest structure, including substrate, ground shrubs and surface fuels, saplings, mid-tier trees, and overstorey canopy and tree crowns (68). Vegetation in these strata were scored according to the vegetation burn assessment module in the BC guidebook that is presented in appendix 1 below. To avoid potential observer bias and ensure the recommended extended assessment was met, CBI surveys were implemented by one researcher (A. Leslie) over two phases in 2015 and in 2019 (67). Aggregated estimates were then used to identify sites of ‘low’, ‘moderate’, and ‘high’ burn severity (66). Using the same Composite Burn Index, aerial post-fire photography was examined for burn effects. Based on levels of scorch within understorey and overstorey vegetation, homogenous burn patches were selected by one photo interpreter (S. Murphy) and digitally coded according to their burn severity using ArcMap (10.7.1). To avoid corruption of Landsat 8 voxels, a minimum diameter of training patches was set at 30m and a minimum boundary spacing between samples of different classes was set at 20m (69). CBI plot samples were digitized and added to the ArcMap manager and the full set of training samples was scanned for violations of homogeneity and pixel corruption using the Measure Tool (70,71).

Training samples were then used to train classification of single-date, post-fire imagery and differenced pre/post-fire imagery (Table 1, Figure 3). Each of the images derived from the 11 burn indices was then classified separately using the following algorithms: Maximum Likelihood Classifier (MLC), Support Vector Machine (SVM), and the Random Tree Classifier (RTC). To compare the accuracy of models, reference data were split 60/40 between training and validation datasets. Randomly selected accuracy points were proportionately stratified between severity classes to enable meaningful confusion matrices (72–74). Kappa values were analysed according to guidelines set out by Tran et al (74,75): “no agreement ($k < 0$); poor agreement (0–0.20); fair agreement (0.21–0.40); moderate agreement (0.41–0.60); substantial agreement (0.61–0.80); and almost perfect agreement (0.81–1.00)”. Results ranged between 0.0062 (Differenced-Char Soil Index (Band 6+)/SVM) to 0.6035 (Differenced-Normalized Burn Ratio (Band 6+)/SVM).

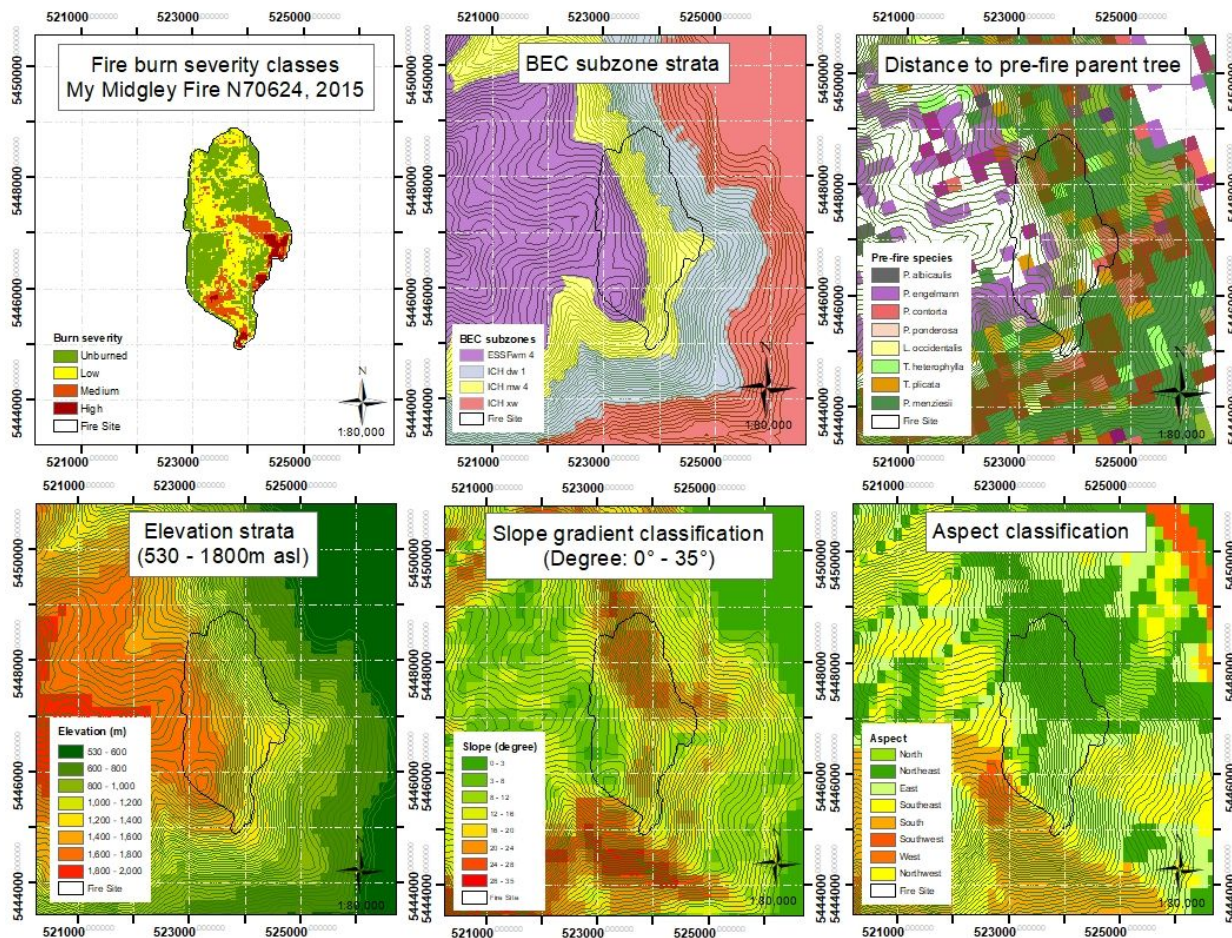
Methods: Variables

Table 1. Predictor variables		Description	Variable type
Fire	1) Burn severity	Burn severity according to CBI plots, D-NBR, SVM, and Landsat 8 imagery	Discrete (Low/High)
	2) Seed source	Distance to parent tree from the stem of the seedling (m)	Continuous
Seedbed	3) Snag wood	Percent (-/+5%) of ground cover comprised of snag wood (<15cm dbh)	Continuous
	4) Shrub/lichen	Percent (-/+5%) of ground cover comprised of shrub, herb or lichens	Continuous
Climate	5) Bare rock	Percent (-/+5%) of ground cover comprised of exposed rock	Continuous
	6) Temperature	Temperature increases of x^*SD of baseline normal values (1981–2011)	Categorical
Topography	7) Precipitation	Geographically weighted mean monthly precipitation (mm/yr, 1981-2019)	Categorical (0.8)
	8) Irradiation	Topographically weighted mean monthly solar irradiation (MJ m ² /yr)	Ordinal (0-8)
Topography	9) Wind	Topographically weighted mean annual wind speed (s/m ²)	Ordinal (0-8)
	10) BEC zone	Seedling location between ESSF, ICHdw1, ICHmw4 ecosystems (BC, 2017)	Categorical (1-3)
Topography	11) Elevation	Seedling elevation (a.s.l. - <i>autocorrelation with BEC above, should we drop?</i>)	Continuous
	12) Slope	Slope gradient of seedbed (degree, 0° - 35°)	Categorical
Topography	13) Aspect	Azimuth aspects weighted and classified using Beers Index (1966)	Categorical
	14) RIX score	Difference in elevation of seedling raster cell and mean neighbour cells	Continuous

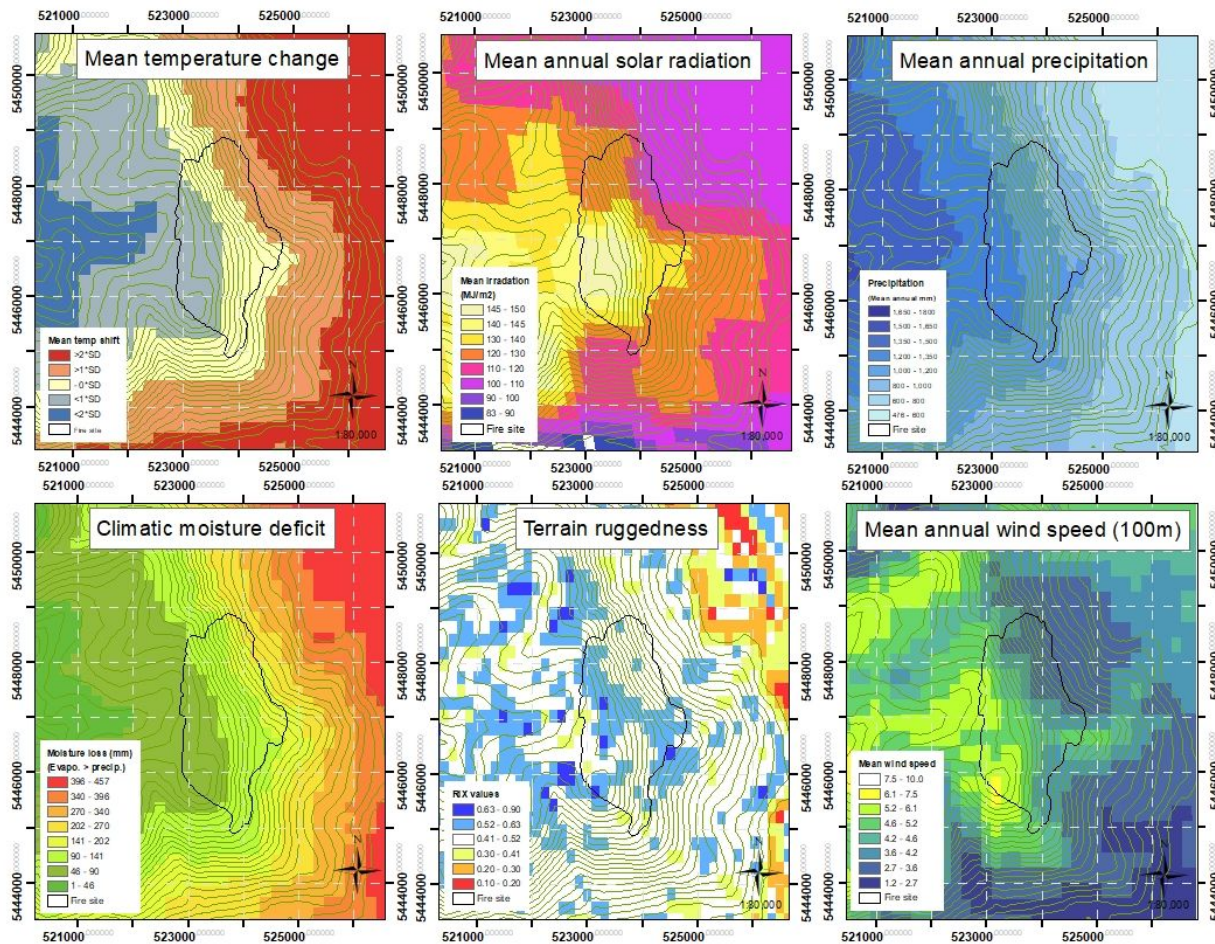
Table 2 Response variables		Description	Variable type
Regeneration	15) Seedling density (#/m ²)	(Between-plot density): Indicator of location-dependent distribution between BEC and fire severity zones in the CSR MPP-model.* (Across-plot density): Indicator of effects of climatic and topographic covariates on logistic intensity of seedling density in the GLMP-model (Within-plot density): Indicator of distance-dependent distribution from seed source in CSR KPP-model.*	Continuous
	16) Seedling height (cm)	(Between-plot density): Indicator of location-dependent patterns between BEC and fire severity zones in the CSR MPP-model.* (Across-plot density): Indicator of effects of climatic and topographic covariates on logistic intensity of seedling height in the GLMP-model (Within-plot density): Indicator of distance-dependent patterns from seed source in CSR KPP-model.*	Continuous

*As described in Owen et al (2018)

Figure 3, Fire severity, location and topography variables



Figures 4, Topography and climatic predictor variables



Appendix I: Data collection forms

12/06/2020

Darkwoods_Wildfire_Regen_2020

Today's Date

yyyy-mm-dd

GPS Location

latitude (x,y *)

longitude (x,y *)

altitude (m)

accuracy (m)

Seedling...

Seedling species?

- Larix occidentalis
- Pseudotsuga menziesii
- Picea engelmannii
- Pinus contorta
- Pinus ponderosa
- Pinus albicaulis
- Thuja plicata
- Tsuga heterophylla

Seedling height?

Questions about fire effects...

Low or high burn severity site?

- Low
- High

Distance to living parent tree?

Questions about seedbed conditions...

Within a 10m radius, what is the percentage of land covered in snag wood (15cm dbh)?

Within a 10m radius, what is the percentage of land covered in shrub, herb or lichen?

Within a 10m radius, what is the percentage of land showing exposed bare rock?

Check topography data...

Which BEC zone are you located?

- ESSF
- ICHdw1
- ICHmw4

What is the current elevation above sea level at this location?

From 0-8, 0 being southwest, 1 west and 8 northeast, which is prevailing azimuth of landscape of surrounding landscape (10m radius)?

<https://kf.kobotoolbox.org/#/forms/a13irfKfxAEQ3sqdyfTLsZX/summary>

Appendix 1; Veg

		Vegetation in natural unburned state	Unburned
Unburned			
Low (green)	Canopy unburned, trunks partially burned, understorey lightly or patchily burned	Low	
Moderate (brown or red)	Trees burned and dead; scorched needles remain on canopy trees, understorey burned and blackened	Moderate	

Unburned	Mostly alive (green)	Mostly dead; needles remaining (brown or red)	Dead; no needles; some twigs and cones (black)	Dead; trunk and large branches only (black)
% Cover: Green understorey: _____ % Green trees: _____ % Brown trees: _____ %				
Vegetation burn severity:	Low	Moderate	High	
Soil burn severity indicator	Indicator class (circle one)			
Litter	scorched, charred	mostly consumed	consumed	
Duff (FH layers)	intact	spottily consumed	mostly consumed	
Woody debris - Small	charred	partly consumed	consumed	
Woody debris - Logs	charred	some consumed	many consumed, others deeply charred	
Ash colour (if present)	black	grey	white	
Mineral soil exposure	<5%	5–40%	>40%	
Change to mineral soil (structure, colour, etc.)	no	minor	yes	
Depth to live roots or rhizomes (in min. soil)	0	0–5 cm	>5cm	

Soil burn severity: Low Moderate High

Size of surrounding areas similar to plot area (table 1) by the number of plots.

Evidence of runoff/overland flow: sand

Water repellency – extent and class:
Results from dripping water along a 0.5–1 m trench exposing the repellent mineral soil layer:
record Water Repellency Class based on the time required for the absorption of a drop of water on

dry soil and % of the trench in that class (Add columns to right if testing more than one depth). Trench depth: _____ cm

a. None - <10 seconds _____ % of trench
 b. Weak - >10 and <40 seconds _____ % of trench
 c. Strong - >40 seconds _____ % of trench

Appendix II: Data collection forms

Bibliography

1. Filmon G. Firestorm 2003. Provincial review of the 2003 fire season. Province of British Columbia; 2004.
2. Hamann A, Wang T. Potential effects of climate change on ecosystem and tree species distribution in British Columbia. *Ecology*. 2006;87(11):2773–86.
3. Waring RH, Coops NC. Predicting large wildfires across western North America by modeling seasonal variation in soil water balance. *Clim Change*. 2016;135(2):325–39.
4. Westerling AL, Hidalgo HG, Cayan DR, Swetnam TW. Warming and earlier spring increase western US forest wildfire activity. *Science* (80-). 2006;313(5789):940–3.
5. Holt F, Utzig G, Pinnell H, Pearce C. Vulnerability, Resilience and Climate Change: Adaptation Potential for Ecosystems and Their Management in the West Kootenay ? Summary Report. Report #1 for the West Kootenay Climate Vulnerability and Resilience Project. 2012.
6. Johnstone JF, Allen CD, Franklin JF, Frelich LE, Harvey BJ, Higuera PE, et al. Changing disturbance regimes, ecological memory, and forest resilience. *Front Ecol Environ*. 2016;14(7):369–78.
7. Utzig G, Holt R, Machmer M. Darkwoods Conservation Property: Climate Change Vulnerability and Fire Management Planning. 2016.
8. Harvey BJ, Donato DC, Turner MG. High and dry: Post-fire tree seedling establishment in subalpine forests decreases with post-fire drought and large stand-replacing burn patches. *Glob Ecol Biogeogr*. 2016;25(6):655–69.
9. Kemp KB, Higuera PE, Morgan P, Abatzoglou JT. Climate will increasingly determine post-fire tree regeneration success in low-elevation forests, Northern Rockies, USA. *Ecosphere*. 2019;10(1):e02568.
10. Kemp KB, Higuera PE, Morgan P. Fire legacies impact conifer regeneration across environmental gradients in the US northern Rockies. *Landsc Ecol*. 2016;31(3):619–36.
11. Tepley AJ, Swanson FJ, Spies TA. Post-fire tree establishment and early cohort development in conifer forests of the western Cascades of Oregon, USA. *Ecosphere*. 2014;5(7):1–23.
12. Bell DM, Bradford JB, Lauenroth WK. Early indicators of change: divergent climate envelopes between tree life stages imply range shifts in the western United States. *Glob Ecol Biogeogr*. 2014;23(2):168–80.
13. Bose AK, Weiskittel A, Wagner RG, Kuehne C. Assessing the factors influencing natural regeneration patterns in the diverse, multi-cohort, and managed forests of Maine, USA. *J Veg Sci*. 2016;27(6):1140–50.

14. Malcolm JR, Markham A, Neilson RP, Garaci M. Estimated migration rates under scenarios of global climate change. *J Biogeogr.* 2002;29(7):835–49.
15. Mathys AS, Coops NC, Simard SW, Waring RH, Aitken SN. Diverging distribution of seedlings and mature trees reflects recent climate change in British Columbia. *Ecol Model.* 2018;384:145–53.
16. Nitschke CR, Innes JL. A tree and climate assessment tool for modelling ecosystem response to climate change. *Ecol Model.* 2008;210(3):263–77.
17. Owen SM, Sieg CH, Meador AJS, Fulé PZ, Iniguez JM, Baggett LS, et al. Spatial patterns of ponderosa pine regeneration in high-severity burn patches. *For Ecol Manage.* 2017;405:134–49.
18. Ziegler JP, Hoffman CM, Fornwalt PJ, Sieg CH, Battaglia MA, Chambers ME, et al. Tree regeneration spatial patterns in ponderosa pine forests following stand-replacing fire: Influence of topography and neighbors. *Forests.* 2017;8(10):391.
19. Wang T. Projecting future distributions of ecosystem climate niches in British Columbia. *J Ecosyst Manag.* 2013;13(3).
20. Fettig CJ, Reid ML, Bentz BJ, Sevanto S, Spittlehouse DL, Wang T. Changing climates, changing forests: a western North American perspective. *J For.* 2013;111(3):214–28.
21. Wang T, Hamann A, Spittlehouse D, Carroll C. Locally downscaled and spatially customizable climate data for historical and future periods for North America. *PLoS One.* 2016;11(6).
22. Dobrowski SZ, Swanson AK, Abatzoglou JT, Holden ZA, Safford HD, Schwartz MK, et al. Forest structure and species traits mediate projected recruitment declines in western US tree species. *Glob Ecol Biogeogr.* 2015;24(8):917–27.
23. Krasowski MJ, Owens JN. Growth and morphology of western red cedar seedlings as affected by photoperiod and moisture stress. *Can J For Res.* 1991;21(3):340–52.
24. Grossnickle SC, Russell JH. Physiological variation among western redcedar (*Thuja plicata* Donn ex D. Don) populations in response to short-term drought. *Ann For Sci.* 2010;67(5):506.
25. Grossnickle SC. Shoot water relations and gas exchange of western hemlock and western red cedar seedlings during establishment on a reforestation site. *Trees.* 1993;7(3):148–55.
26. Zhang J, Marshall JD. Population differences in water-use efficiency of well-watered and water-stressed western larch seedlings. *Can J For Res.* 1994;24(1):92–9.
27. Sparks AM, Talhelm AF, Feltrin RP, Smith AMS, Johnson DM, Kolden CA, et al. An experimental assessment of the impact of drought and fire on western larch injury, mortality and recovery. *Int J Wildl Fire.* 2018;27(7):490–7.
28. Oswald BP, Neuenschwander LF. Microsite variability and safe site description for western larch

- germination and establishment. *Bull Torrey Bot Club*. 1993;148–56.
- 29. Arno SF, Davis DH. Fire history of western redcedar/hemlock forests in northern Idaho. In: Proceedings of the Fire History Workshop Gen Tech Rep RM-81 USDA For Serv, Rocky Mountain Forest and Range Exp Sta, Fort Collins, CO. 1980. p. 21–6.
 - 30. Rother MT. Conifer regeneration after wildfire in low-elevation forests of the Colorado Front Range: implications of a warmer, drier climate. 2015;
 - 31. Burns RM. Silvics of North America: Conifers. US Department of Agriculture, Forest Service; 1990.
 - 32. Elliott GP, Kipfmüller KF. Multi-scale influences of slope aspect and spatial pattern on ecotonal dynamics at upper treeline in the southern Rocky Mountains, USA. *Arctic, Antarct Alp Res*. 2010;42(1):45–56.
 - 33. Thomas PA, Wein RW. The influence of shelter and the hypothetical effect of fire severity on the postfire establishment of conifers from seed. *Can J For Res*. 1985;15(1):148–55.
 - 34. Resler LM, Butler DR, Malanson GP. Topographic shelter and conifer establishment and mortality in an alpine environment, Glacier National Park, Montana. *Phys Geogr*. 2005;26(2):112–25.
 - 35. Blanco JA, Welham C, Kimmins JP, Seely B, Mailly D. Guidelines for modeling natural regeneration in boreal forests. *For Chron*. 2009;85(3):427–39.
 - 36. Weiskittel AR, Hann DW, Kershaw Jr JA, Vanclay JK. Forest growth and yield modeling. John Wiley & Sons; 2011.
 - 37. Parmesan C, Duarte C, Poloczanska E, Richardson AJ, Singer MC. Overstretching attribution. *Nat Clim Chang*. 2011;1(1):2–4.
 - 38. Larson AJ, Churchill D. Tree spatial patterns in fire-frequent forests of western North America, including mechanisms of pattern formation and implications for designing fuel reduction and restoration treatments. *For Ecol Manage*. 2012;267:74–92.
 - 39. Agee JK. Fire ecology of Pacific Northwest forests. Island press; 1996.
 - 40. Agee JK. The landscape ecology of western forest fire regimes. *Northwest Sci*. 1998;72(17):24–34.
 - 41. Agee JK. Historical range of variability in eastern Cascades forests, Washington, USA. *Landsc Ecol*. 2003;18(8):725–40.
 - 42. Donato DC, Fontaine JB, Campbell JL, Robinson WD, Kauffman JB, Law BE. Conifer regeneration in stand-replacement portions of a large mixed-severity wildfire in the Klamath-Siskiyou Mountains. *Can J For Res*. 2009;39(4):823–38.

43. Dave K, Douglas J. Patch Retention Harvesting as a Technique for Maintaining Stand Level Biodiversity in Forests of North Central British Columbia. *Proc Innov Silvic Syst Boreal For.* 2009;102.
44. Woolsey TS. Western yellow pine in Arizona and New Mexico. US Department of Agriculture, Forest Service; 1911.
45. Munger TT. Western yellow pine in Oregon. US Department of Agriculture; 1917.
46. Meyer HA. Eine mathematisch-statistische Untersuchung über den Aufbau des Plenterwaldes. Buchler & Company; 1933.
47. Cooper CF. Pattern in ponderosa pine forests. *Ecology.* 1961;42(3):493–9.
48. Pielou EC. A single mechanism to account for regular, random and aggregated populations. *J Ecol.* 1960;575–84.
49. Pielou EC. Segregation and symmetry in two-species populations as studied by nearest-neighbour relationships. *J Ecol.* 1961;255–69.
50. Pielou EC. The use of plant-to-neighbour distances for the detection of competition. *J Ecol.* 1962;357–67.
51. Bonnet VH, Schoettle AW, Shepperd WD. Postfire environmental conditions influence the spatial pattern of regeneration for *Pinus ponderosa*. *Can J For Res.* 2005;35(1):37–47.
52. Baddeley A, Diggle PJ, Hardegen A, Lawrence T, Milne RK, Nair G. On tests of spatial pattern based on simulation envelopes. *Ecol Monogr.* 2014;84(3):477–89.
53. Boyden S, Binkley D, Shepperd W. Spatial and temporal patterns in structure, regeneration, and mortality of an old-growth ponderosa pine forest in the Colorado Front Range. *For Ecol Manage.* 2005;219(1):43–55.
54. Malone SL, Fornwalt PJ, Battaglia MA, Chambers ME, Iniguez JM, Sieg CH. Mixed-severity fire fosters heterogeneous spatial patterns of conifer regeneration in a dry conifer forest. *Forests.* 2018;9(1):45.
55. Dale MRT, Fortin M-J. *Spatial analysis: a guide for ecologists.* Cambridge University Press; 2014.
56. MacKenzie WH, Meidinger D V. The Biogeoclimatic Ecosystem Classification Approach: an ecological framework for vegetation classification. *Phytocoenologia.* 2018;48(2):203–13.
57. Boe KN. *Silvics of western larch.* Intermountain Forest and Range Experiment Station, Forest Service, US~...; 1958.
58. Schmidt WC, Shearer RC. *Larix occidentalis* Nutt. western larch. *Silvics North Am Conifers.*

- 1990;(654):160.
59. Tubbs CH, Houston DR. US Department of Agriculture, Forest Service. 1965. Silvics of forest trees of the United States. HA Fowells, comp. US Dep Agric Agric Handb. 1965;271.
 60. Schmidt WC. Seedbed treatments influence seedling development in western larch forests. Vol. 93. US Dept. of Agriculture, Forest Service, Intermountain Forest & Range~...; 1969.
 61. Beaudoin A, Bernier PY, Guindon L, Villemaire P, Guo XJ, Stinson G, et al. Mapping attributes of Canada's forests at moderate resolution through k NN and MODIS imagery. *Can J For Res*. 2014;44(5):521–32.
 62. Riley SJ, DeGloria SD, Elliot R. Index that quantifies topographic heterogeneity. *Intermt J Sci*. 1999;5(1–4):23–7.
 63. Amatulli G, Domisch S, Tuanmu M-N, Parmentier B, Ranipeta A, Malczyk J, et al. A suite of global, cross-scale topographic variables for environmental and biodiversity modeling. *Sci data*. 2018;5:180040.
 64. Daly C, Helmer EH, Quiñones M. Mapping the climate of puerto rico, vieques and culebra. *Int J Climatol A J R Meteorol Soc*. 2003;23(11):1359–81.
 65. Hope G d'Egville. Post-wildfire natural hazards risk analysis in British Columbia. BC Ministry of Forests and Range, Forest Science Program; 2015.
 66. Key CH, Benson NC. Landscape assessment: remote sensing of severity, the normalized burn ratio and ground measure of severity, the composite burn index. FIREMON Fire Eff Monit Invent Syst Ogden, Utah USDA For Serv Rocky Mt Res Stn. 2005;
 67. Parks SA, Dillon GK, Miller C. A new metric for quantifying burn severity: the relativized burn ratio. *Remote Sens*. 2014;6(3):1827–44.
 68. Collins L, Griffioen P, Newell G, Mellor A. The utility of Random Forests for wildfire severity mapping. *Remote Sens Environ*. 2018;216(June):374–84.
 69. Parson A, Robichaud PR, Lewis SA, Napper C, Clark JT. Field guide for mapping post-fire soil burn severity. Gen Tech Rep RMRS-GTR-243 Fort Collins, CO US Dep Agric For Serv Rocky Mt Res Station 49 p. 2010;243.
 70. Walz Y, Maier SW, Dech SW, Conrad C, Colditz RR. Classification of burn severity using Moderate Resolution Imaging Spectroradiometer (MODIS): A case study in the jarrah-marri forest of southwest Western Australia. *J Geophys Res Biogeosciences*. 2007;112(G2).
 71. Sparks AM, Kolden CA, Talhelm AF, Smith A, Apostol KG, Johnson DM, et al. Spectral indices accurately quantify changes in seedling physiology following fire: towards mechanistic assessments of post-fire carbon cycling. *Remote Sens*. 2016;8(7):572.

72. Kolden CA, Smith AMS, Abatzoglou JT. Limitations and utilisation of Monitoring Trends in Burn Severity products for assessing wildfire severity in the USA. *Int J Wildl Fire*. 2015;24(7):1023–8.
73. Tran BN, Tanase MA, Bennett LT, Aponte C. Evaluation of spectral indices for assessing fire severity in Australian temperate forests. *Remote Sens*. 2018;10(11):1680.
74. Holle H, Rein R. The modified Cohen's kappa: Calculating interrater agreement for segmentation and annotation. *Underst Body Mov A Guid to Empir Res Nonverbal Behav* H Lausberg, Ed Frankfurt am Main Peter Lang Verlag. 2013;261–77.
75. MacKillop D, Ehman A. *A Field Guide to Ecosystem Classification and Identification for Southeast British Columbia*. 2016.
76. Meidinger D, Pojar J. *Ecosystems of British Columbia*. Research Branch, Ministry of Forests. Br Columbia, Victoria. 1991;